Syntheses, studies and crystal structure of new coordination polymers of mercury (II) with phenylcyanamide derivative ligands

Hossein Chiniforoshan, Nasimeh Pourrahim, Leila Tabrizi, Hossein Tavakol, Mohammad R. Sabzalian, Behrouz Notash

PII: S0020-1693(14)00161-3
DOI: http://dx.doi.org/10.1016/j.ica.2014.03.016
Reference: ICA 15916

To appear in: *Inorganica Chimica Acta*

Received Date: 12 December 2013
Revised Date: 25 February 2014
Accepted Date: 9 March 2014

Please cite this article as: H. Chiniforoshan, N. Pourrahim, L. Tabrizi, H. Tavakol, M.R. Sabzalian, B. Notash, Syntheses, studies and crystal structure of new coordination polymers of mercury (II) with phenylcyanamide derivative ligands, *Inorganica Chimica Acta* (2014), doi: http://dx.doi.org/10.1016/j.ica.2014.03.016

Syntheses, studies and crystal structure of new coordination polymers of mercury (II) with phenylcyanamide derivative ligands

Hossein Chiniforoshan[*a], Nasimeh Pourrahim[a], Leila Tabrizi[a], Hossein Tavakol[a], Mohammad R. Sabzalian[b], Behrouz Notash[c].

[a]*Department of Chemistry, Isfahan University of Technology, Isfahan 84156-83111, Iran*
[b]*Department of Agronomy and Plant Breeding, College of Agriculture, Isfahan University of Technology*
[c]*Department of Chemistry, Shahid Beheshti University, Evin, Tehran 1983963113, Iran*

Abstract

A series of compounds mercury (II), $[Hg(CH_2COCH_3)L]_n$ where L= anion of 4-NO_2pcyd (4-nitro phenylcyanamide) (**1**), 4-Clpcyd (4-chloro phenylcyanamide) (**2**), 4-Brpcyd (4-bromo phenylcyanamide) (**3**) were synthesized from acetone and characterized by elemental analysis, IR, ^{1}H NMR, ^{13}C NMR and electronic absorption spectroscopies. Single crystal X ray analysis of **1** reveals coordination of phenylcyanamide ligand to Hg (II) unexpectedly occurred through amine nitrogen alone which is rare. Also the anion of acetone was coordinated to mercury by the carbon atom as well as oxygen atom from (C=O) of another acetone anion. A theoretical study at DFT (B3LYP) level showed that the experimentally determined structure of the complex **1** is about 6.49kcal/mol and 8.31kcal/mol, respectively in the gas phase and solvent more stable than its other bonding modes. In addition, this phenomenon was supported by NBO interaction energies and the much orbital contribution in the HOMO of ligand to interact with Hg (II) that all of these observations were raised from the presence of nitro group as electron withdrawing group. By using TD-DFT method, electronic absorption spectra of the compound **1** have been predicted and a good agreement with the TD-DFT method and the experimental one is determined. Biological studies show the antibacterial activity of the complex **1** against Gram-positive and Gram-negative bacterial strains.

*Corresponding author: H. Chiniforoshan; Email: Chinif@cc.iut.ac.ir
Tel: +983113913261; fax: +983113912350

Keywords: Mercury (II) complex; Coordination polymer; Phenylcyanamide; NMR spectra, Theoretical calculation, Antibacterial agent.

1. Introduction

Coordination polymers of organomercury derivatives are widely investigated in recent years, not only for their potential applications [1–3] but also for their attractive flexibility in building up extended structures [4–7]. Coordination polymers based on the soft Hg (II) ion are much less predictable in respect to coordination number at the metal [8] and represent a synthetic challenge to crystal engineering.

In some respects, anionic phenylcyanamides behave as pseudohalides in their ligating properties. However, the attachment of a phenyl ring to the cyanamide group (NCN) adds an extra dimension not present in azide or thiocyanate ligands. An extensive π conjugation between the cyanamide group and the phenyl ring provides an energetically favorable means by which a metal ion can couple into a conjugated organic π system [9]. And so, overall, they are ambidentate in nature exhibiting three different coordination modes, namely (i) monodentate via the cyano nitrogen, (ii) μ-1,3-bridging through both the amino and cyano nitrogens and (iii) μ-1,1-bridging via the cyano nitrogen [10]. The amine nitrogen is sterically crowded by the phenyl ring and so terminal coordination to the cyano nitrogen is expected. There are many crystal structures of monodentate phenylcyanamide ligands showing coordination through the cyano nitrogen but there were a few examples of amine nitrogen coordination that coordinate through the amine alone [11]. In this study, a series of novel polymer complexes of the of $[Hg(CH_2COCH_3)L]_n$, where L=4- nitro phenylcyanamide (4-NO_2pcyd) (**1**), 4-chloro phenylcyanamide (4-Clpcyd) (**2**), 4-bromo phenylcyanamide (4-Brpcyd) (**3**), a phenylcyanamide anion ligand, has been synthesized and characterized by IR, ^{1}H NMR and ^{13}C NMR spectroscopies and it has been shown that coordination of phenylcyanamide ligand to Hg (II) unexpectedly occurred through amine nitrogen alone

which is rare [11]. Another interesting phenomenon in this study is formation of an organometallic compound that has been produced by linkage of the terminal anionic carbon atom of acetone to a metal ion. A crystal structure determination of the complex $[Hg(CH_2COCH_3)(4\text{-}NO_2pcyd)]_n$ as well as the density functional theory (DFT) has been performed. We also make comparisons between experiments and calculations. Also antibacterial assay over Gram-positive and Gram-negative pathogenic bacterial strains was studied.

2. Experimental section

2.1. Materials

The phenylcyanamide ligands were prepared in air according to the literature procedure [12] and used without further purification. All chemicals and solvents were highly pure Merck compounds and used without any further purification.

Caution! Mercury and its compounds are toxic [13].

2.2. Methods and Instrumentation

Fourier transform infrared spectra were recorded on a FT-IR JASCO 680-PLUS spectrometer in the region of 4000–400 cm^{-1} using KBr pellets. Electronic spectra were obtained using a UV-JASCO-570 spectrometer. ^1H NMR and ^{13}C NMR spectra were recorded on a Bruker DRX-500 MHz Avance spectrometer at 100 K in DMSO-d_6 with tetramethylsilane (TMS; δ = 0 ppm) as internal standard. Elemental analyses were performed by using a Leco, CHNS-932 elemental analyzer.

2.3 X-ray structural determination of $[Hg(CH_2COCH_3)(4\text{-}NO_2pcyd)]_n$ (1)

A yellow needle crystal with a dimension of 0.28×0.18×0.10 mm^3 was mounted on a glass fiber and used for data collection. All measurements were made on a STOE IPDS-II diffractometer with graphite monochromated Mo Kα radiation. Cell constants and an

orientation matrix for data collection were obtained by least-squares refinement of diffraction data from 6799 unique reflections. Data were collected at a temperature of 298(2)K to a maximum 2Θ value of 58.4 and in a series of ω scans in 1° oscillations and integrated using the STOE X-AREA software package [14]. A numerical absorption correction was applied using X-RED [15] and X-SHAPE [16] software's. The data were corrected for Lorentz and Polarizing effects. The structure was solved by direct methods [17] and subsequent difference Fourier maps and then refined on F^2 by a full-matrix least-squares procedure using anisotropic displacement parameters [16]. All of hydrogen atoms were located in a difference Fourier map and thereafter refined isotropically. Crystallographic data and details of the data collection and structure refinements are listed in Table 1.

Table1.

2.4. Synthesis of mercury (II) complexes

2.4.1. $[Hg(CH_2COCH_3)(4\text{-}NO_2pcyd)]_n$ (1)

The ligand of 4-NO_2-pcyd (0.2 mmol, 33 mg) was deprotonated by reaction with NaOH (0.4 mmol, 16 mg) in acetone (10 ml) with stirring at reflux temperature overnight. The resulting solution was added to a stirred solution of $Hg(NO_3)_2.H_2O$ (0.2 mmol, 68 mg) in acetone (15 ml) and the reaction mixture was stirred at reflux temperature for 4 hours and then the resulting reaction mixture left at room temperature and allowed to air dry. Yellow crystals of $[Hg\ (CH_2COCH_3)(4\text{-}NO_2pcyd)]_n$ were grown after days. Yield: 65%. Anal. Calc. (%): C, 28.61; H, 2.16; N, 10.01; and Found (%): C, 28.59; H, 2.14; N, 9.98. Selected FT-IR data, ν(cm^{-1}): ν(C≡N): 2140(vs), ν(CO): 1726.3(vs), ν(NO_2):1590.02, 1310.39(s), ν(C–N): 1125(m) (see Supplementary material). ^{1}H-NMR (DMSO): 1.18(s, 3H), 2.14 (s, 1H), 2.61 (s, 1H), 6.82 (d, 2H), 7.62(d, 2H) ppm. ^{13}C–{^{1}H} NMR (DMSO): 30.25(CH_3),

56.41(CH_2), 120.10(C7), 124.13(C2,6), 126.75(C4), 131.90(C3,5), 153.04(C1) and 216.90(CO) ppm (Scheme1).

2.4.2. $[Hg(CH_2COCH_3)(4\text{-}Clpcyd)]_n$ (2)

Complex **2** was prepared in a similar way to **1** with the use of ligand of 4-Cl-pcyd (0.2 mmol, 30.5mg) instead of 4-NO_2-pcyd. The white solid obtained was vacuum filtered, washed with acetone, and dried in desiccator over $CaCl_2$. Yield: 77%. Anal. Calc. (%): C, 29.35; H, 2.22; N, 6.85; and Found (%): C, 29.33; H, 2.19; N, 6.81. Selected FT-IR data, ν(cm^{-1}): ν(C≡N): 2190(vs), ν(CO): 1728.2(vs), ν(C–N): 1165(m) (see Supplementary material). ^{1}H-NMR (DMSO): 1.15(s, 3H), 2.12 (s, 1H), 2.49 (s, 1H), 6.65 (d, 2H), 6.98(d, 2H) ppm. ^{13}C–{^{1}H} NMR (DMSO): 30.20(CH_3), 56.38(CH_2), 119.03(C7), 120.12(C2,6), 126.56(C4), 128.66(C3,5), 152.70(C1) and 216.65(CO) ppm (Scheme1).

2.4.3. $[Hg(CH_2COCH_3)(4\text{-}Brpcyd)]_n$ (3)

Complex **3** was prepared in a similar way to **1** with the use of ligand of 4-Br-pcyd (0.2 mmol, 39.4mg) instead of 4-NO_2-pcyd. The white solid obtained was vacuum filtered, washed with acetone, and dried in desiccator over $CaCl_2$. Yield: 70%. Anal. Calc. (%): C, 26.47; H, 2.00; N, 6.17; and Found (%): C, 26.45; H, 1.97; N, 6.14. Selected FT-IR data, ν (cm^{-1}): ν(C≡N): 2183(vs), ν(CO): 1725.4(vs), ν(C–N): 1070(m) (see Supplementary material). ^{1}H-NMR (DMSO): 1.16(s, 3H), 2.10 (s, 1H), 2.57 (s, 1H), 6.68 (d, 2H), 7.14(d, 2H) ppm. ^{13}C–{^{1}H} NMR (DMSO): 30.21(CH_3), 56.29(CH_2), 107.57(C7), 120.96(C2,6), 126.44(C4), 131.64(C3,5), 151.94(C1) and 216.10(CO) ppm (Scheme1).

2.5. Computational methods

The geometry optimizations, frequency calculations (including energies) and population analyses were performed employing Gaussian 09 program package [18]. In addition, natural

bond orbital calculations (NBO) were used to obtain the natural atomic charges and second-order perturbation energies (to estimate the values of intermolecular interactions) [19]; this method is implemented in the Gaussian program package. Solvent effects in acetone (reaction solvent) were determined by calculation of free energies of solvation using SCRF keyword at Tomasi's polarized continuum (PCM) model [20]. All calculations were performed using DFT calculations at CAM-B3LYP/6-311+G* level of theory and carried out at room temperature and standard pressure. Time-dependent density functional theory (TD-DFT) calculations were employed to obtain the computational UV-Vis spectra of complex **1** and these calculations were performed at TD CAM-B3LYP/6-311+G* level of theory. The theoretical data were obtained after optimization of the molecular geometry without any symmetry restriction.

2.6. Anti bactericidal assay

The free ligand of 4-NO_2-pcyd and metal complex (**1**) were screened for their antimicrobial activities against *E.coli* (Enterobacteriaceae) as the model from Gram-negative bacteria and *Salmonella aureus* (Staphylococcaceae) as the model from Gram-positive bacteria by the disc diffusion method. The method was designed to test the ability of antimicrobial agents quickly and qualitatively in order to inhibit the growth of microorganisms over a short period of time. After incubation, usually overnight or after a few days, a circular inhibition zone of microbial growth appears around the disc of material as a result of antibiotic diffusion into the agar and growth inhibition of the bacterial isolates. The zone sizes are compared and the bacterial isolate is recorded as sensitive, intermediate or resistant to the applied material [21-23].

2.6.1. Preparation of Nutrient - Agar Medium

To prepare one litre of Nutrient-Agar (NA) medium, 5 g of peptone, 3 g of meat extract, 5 g NaCl and 15 g agar were dissolved in 1000 ml of distilled water. The solution was sterilized at 120 ° C for 20 min in an autoclave, and then 20 ml of culture medium was solidified in

each 35 cm Petri plate.

2.5.2. The inhibition zone test (disc diffusion method)

A microbial suspension (1 ml) of *E. coli* and *Salmonella aureus* was spread evenly over the surface of nutrient agar plate (bacterial concentration was measured to be 10^8 per 50 micro-liters). The ligand of 4-NO_2-pcyd or metal complex (**1**) was separately applied to the centre of agar plates as a disc with 12 mm diameter (10 mg of each) in three replicates (in a fashion that the material doesn't spread out from the centre). Agar plates were then incubated for one week at 25±2 ˚C and inhibition zone was monitored. The size of inhibition zone (diameter of inhibition) was related to the level of antimicrobial activity present in the products.

3. Results and discussion

3.1. Synthesis and characterization

Phenylcyanamide derivatives can be readily prepared in high yields from the corresponding anilines [12]. The polymer complexes of $[Hg(CH_2COCH_3)L]_n$, (L=4-NO_2pcyd, 4-Clpcyd, 4-Brpcyd), have been prepared by the deprotonation of phenylcyanamide with sodium hydroxide in acetone and the addition of this solution to a solution of $Hg(NO_3)_2.H_2O$ in acetone. The infrared data for the anion of phenylcyanamide ligands and complexes of Hg (II) are listed in Table 2 (data provided as Supplementary material). The identification of C-N vibrations is a very difficult task, since mixing of several bands is possible in this region. Silverstein and Webster [24] assigned C-N stretching absorption in the region 1382–1266 cm^{-1} for aromatic amines. In the present, the bands observed in the region 1300–1100 cm^{-1} in FT-IR spectrum have been assigned to C-N stretching vibrations. When the anion of phenylcyanamide ligand coordinates to Hg (II), ν(C-N) is shifted to lower energies. The ν(C≡N) bands observed in the region 2140–2190 cm^{-1} (Table 2) but there is no much difference between the bands of the anion of ligand and the complexes suggesting the

importance of coordination of cyanamide via the amine nitrogen and locking in the negative charge on the amine nitrogen. The ν (CO) appears at higher frequencies in comparison with the parent acetone (1716 cm^{-1}) which is in agreement with the shortening observed in the C=O distance in complexes [25-27].

The protons NMR spectra of the pcyd ligands and complexes **1**-**3** (see Table 3) in DMSO-d_6 were clean and easily assigned. Up on coordination of pcyd ligands to Hg (II) the proton chemical shifts decrease with respect to the free ligands. The protons of the methylene group are not equivalent due to differences in their chemical environment when carbon is bonded to mercury.

Table2.

Table3.

The ^{13}C NMR spectrum of ligands and complexes in DMSO-d6 were also recorded (see Table 4). The numbering for ^{13}C-NMR data and $pcyd^-$ derivatives is shown in scheme 1. The most interesting aspect of the ^{13}C NMR spectra of the complexes is the shifts observed in the carbons of nitrile and amine signals with respect to the free ligands, which indicate coordination through the NCN group. The ^{13}C NMR shifts of the CO group in complexes are around 216 ppm, at a lower field than around 206 ppm noted for the same carbon in the parent acetone, indicating much lower shielding of carbon of the CO group in these complexes.

Electronic spectral data for the Hg (II) complexes in DMF are assembled in Table 5. The bands in the region 260-270 and 400-450 nm correspond closely to ligand-centered $\pi \rightarrow \pi^*$ transitions [9,28,29]. In this study, the experimentally observed spectra of complex **1** showed two bands at 267 nm (log ε = 3.18) and 451 (log ε = 3.85) nm. Electronic absorption spectra of the compound **1** was calculated by the TD-DFT method based on the TD CAM-B3LYP/6-311+G* level optimized structure in gas phase. For TD-DFT calculations, the theoretical

absorption bands are obtained at 446 nm with oscillator strength being 0.0195 and 274nm with oscillator strength being 0.024 and can easily be seen that they correspond to the experimental absorption ones.

scheme1

Table4.

Table5.

3.2. Structure description of 1

A crystal structure determination of the complex $[Hg(CH_2COCH_3)(4\text{-}NO_2pcyd)]_n$ has been performed and ORTEP diagram of the complex is shown in Fig.1. The anions of the phenylcyanamide ligand and acetone solvent are coordinated to the Hg (II) ion. The cyanamide group binds to Hg (II) only through the amine nitrogen and the acetone is coordinated via carbon atom [C(8)]. The cyanamide groups are almost in the plane of the benzene ring due to strong π-coupling between them. In addition, a bond length of 1.37(2)Å between the amine nitrogen of cyanamides and aromatic carbon [C(2)-N(2)] suggests a great deal of double-bond character and strong π interaction between the cyanamide groups and the benzene ring. The bond angle formed by those atoms [C(8)-Hg-N(2)] is 175.6(7)˚ and the NCN moiety is almost linear with the [N(1)-C (1)-N(2)] angle of 174(2)˚. Bond angles around [C(2)-N(2)-C(1)], [C(2)-N(2)-Hg], [C(1)-N(2)-Hg] are 118.8(17)˚, 124.2(13)˚, 116.2 (13)˚ respectively and are close to 120˚ with the summation of the angles being 359.2˚ which it has been in-plane. The dihedral angle between two planes of phenyl ring and [C(2)-C(1)-N(2)-Hg] equals to 4.99˚ which shows an approximately planar structure. This suggests that the amine nitrogen atoms make the connection by the double bond. Bond angle around [C(2)-N(2)-Hg] is 124.2(13)˚, but as we expected bond angle around [C(1)-N(1)-Hg] unit is almost linear with an angle close to 180˚ [11] that has less inhibition than the first. So we defined two isomer b1 (bond of N(2)-Hg) and b2 (bond of N(1)-Hg) for determining theoretically

whether b1 is the major isomer and the reasons for this preference. The bond length [C(1)-N(1)] and [C(2)-N(2)] is, respectively, 1.17 and 1.37Å. The C ≡ N bond length of nitrile and the C = N bond length of imine group are respectively 1.136 and 1.279Å [30]. So, the bond C(1)-N (1) is a quasi-triple bond and C(2)-N(2) is a quasi-double which is due to resonance between the phenyl ring and N(2)-C(1)-N(1) moiety. Packing diagram of complex**1** indicates 1D polymeric structure which Hg (II) centers in the polymers is three coordinated but with T-shape coordination environment (see Fig.2), which is a common coordination type in mercury chemistry [31,32]. The mercury atom is surrounded by one nitrogen atom of imine from phenylcyanamide ligand with Hg–N distance of 2.120(17) Å and one carbon atom of the acetone ligand with Hg–C distances of 2.097(19) Å and also one oxygen atom of from (C=O) of another acetone anion with Hg–O distances of 2.820 (17) Å. The resulting Hg-O distance of 2.820(17) Å is much shorter than the sum of the van der Waals radii for mercury (rvdw = 1.75 Å) [33] and oxygen (rvdw = 1.54 Å) [34] which indicating the presence of significant bonding interactions between the mercury atom and the oxygen atom of acetone in the molecular structure. Fractional atomic coordinates and equivalent isotropic displacement coefficients (U_{eq}) for the non-hydrogen atoms of complex **1** are shown in Table S1 (Supplementary material).Table 6 lists key bond lengths and angles for complex**1**.

Fig.1.

Fig.2.

Table6.

3.3. Theoretical studies

Complex **1** has two isomers, b1 and b2, that are presented in Fig.3 in attendant with the numbering scheme of the studied molecules. The isomer b1 is the unique isomer that was characterized by X-ray crystal structure analysis. Of interest will be to determine theoretically whether this is the major isomer and the reasons for this preference. In the b1 isomer, the

ligand (4-NO_2pcyd, a) acts via amine nitrogen (N2) and in b2 isomer, the cyano nitrogen (N1) binds to the metal. Our calculation showed that in gas phase and solvent (acetone, the solvent of the reaction), b1 is the major isomer and it is more stable than b2 by 6.49kcal/mol and 8.31kcal/mol, respectively in the gas phase and solvent. In addition to the calculated stabilities, the para-nitro group is electron withdrawing group and adsorbs the electron density of NCN toward the benzene ring and electron density is located on N2 more than N1 and the N2 is complexed to Hg, not N1. To make more insight about these isomers, molecular parameters (bond lengths (Å) and bond angles) were extracted from the optimized structures and compared with the observed X-Ray data in Table 7. Table shows that calculated parameters of isomer b1 are in better agreement with the structure observed by X-ray crystallography, although the calculated bond lengths are slightly different from measured ones. Moreover, the value of the C(1)-N(2)-C(2)-C(3) dihedral angle (shown in the last rows of the table) confirm planarity of the molecules.

NBO calculations are useful tools to calculate molecular properties such as precise atomic charges (Table 8) and the interactions between important parts of molecules (second-order perturbation energies, Table 9) with high precision. Table 8 presents natural atomic charges in ligand (a) in addition to those for both isomers of complex **1** (b1 and b2). It is noticeable that in ligand, more negative charge placed on N2 (-0.362 au) versus N1 (-0.337) that shows why the complexation occurred at N2. In addition, in isomer b1, the absolute value of the charge placed on the N2 atom is larger than that in the isomer b2. This shows that there is a more effective interaction between the N2 atom and mercury rather than the N1 atom and mercury. In Table 9, the most important interaction between ligand and mercury, obtained from NBO second order perturbation energies (E2) are listed. These types of data are a criterion of interaction strength in studied molecules. In our molecules, both important interactions (lone pair of N to Hg and lone pair of N to σ*(Hg-C)) have remarkable larger

values in b1 versus b2. Therefore, since the strength of interaction between metal ion and ligand is one of the factors that helpful in determining the stability of the studied complex, these values confirm that in b1, the efficiency of this interaction is greater than that in b2.

In order to reveal the further coordinating interaction behaviors between ligand and Hg (II), the frontier molecular orbitals and their density distribution analysis in ligand and two isomers were presented. In the coordination process, the ligand is a Lewis base (electron pair donor), while the Hg (II) acts as a Lewis acid (an electron pair acceptor). According to the Frontier Molecular Orbital Theory (FMO theory) [35–37], the occupied orbitals of ligand interact with the unoccupied orbitals of the Hg (II). E_{HOMO} measures the electron donating character of a compound, while E_{LUMO} measures its electron accepting character. Thus, the greater the E_{HOMO} is, the greater the electron donating capability will be, and the smaller the E_{LUMO} is, the smaller the resistance to accept electrons will be. Fig.4 shows HOMO and LUMO molecular orbitals for ligand and both isomers of complex **1**. For the more stable isomer (b1), E_{LUMO} is low (-0.015 eV), whereas in the unstable isomer b2 has large value, -0.024 eV. As a result, two isomers (b1 and b2) have the same HOMO level and since the LUMO level of b1 is lower than b2, so isomer b1 is more stable than b2. Also our calculation shows that in the HOMO of ligand, the contribution of the 2p orbital of nitrogen for N1 is 0.438 and for N2 is 0.608 and hence N2 has more contribution in HOMO. We know that based on basic fundamentals of chemistry, each atom (or orbital) has the much contribution in HOMO, this atom is the major place to start the nucleophilic attack and therefore it has more effective interaction with Hg (II). All of these observations were raised from the presence of nitro group as electron withdrawing group and show why b1 is the major isomer.

Fig.3

Fig.4

Table7.

Table8.

Table9.

3.4. Antibacterial assay

The results of the antibactericidal assay showed that the 4-NO_2pcyd and complex**1** exhibited a large inhibition zone indicating their antibacterial properties (Fig.5) and the inhibitory zone values (mm) are summarized in Table 10. Generally, the diameter of inhibition zone was more than 30 mm in both of 4-NO_2-pcyd and Hg (II) complex (**1**) in *E-coli* and *Salmonella* (Table 10), which represent probable sensitiveness of both Gram-negative and Gram-positive bacteria to the compounds. Gwaram et al. [38] studying antibacterial effects of some synthetic Schiff bases derived from 2-Acetylpyridine and their metal complexes against *Salmonella aureus* showed that the diameter of inhibition zone around the impregnated discs was more than 20 mm in some compounds.

Fig.5

Table10.

4. Conclusion

In the present work, we have synthesized and characterized three Hg (II) complexes of phenylcyanamide derivatives, **1**–**3**, and emphasis has been given to coordination of phenylcyanamide ligand to Hg (II) through amine nitrogen alone which is rare. Also, the anion of acetone was coordinated to mercury by the carbon atom as well as oxygen atom from (C=O) of another acetone anion. X-ray crystal structure indicates 1D polymeric structure with the Hg (II) centers in the polymers having a three coordinated T-shape environment with the third position being taken up by an oxygen atom. The resulting Hg-O distance is much shorter than the sum of the van der Waals radii for mercury and oxygen indicating the presence of significant bonding interactions between the mercury atom and the

oxygen atom of acetone in the molecular structure. The result of theoretical study on the gas and solvent phase showed that the experimentally determined structure of the complex **1** is more stable than its other bonding modes that the para-nitro group as electron withdrawing group is responsible for this phenomenon. The TD-DFT calculations of complex **1** lead to a close agreement with the experimental absorption spectra in gas phase. The ligand of 4-NO_2pcyd and its complex were tested against Gram-positive (*Salmonella aureus*) and Gram-negative bacteria (*E.coli*).The growth inhibition ring of *E.coli* and *Salmonella* was observed in both, showing dramatic antibacterial effectiveness of complex **1** against two bacterial species.

Acknowledgements

We are grateful for the financial support from the Department of Chemistry, Isfahan University of Technology (IUT).

Appendix A. Supplementary data

CCDC 974122 contains the supplementary crystallographic data for compound **1**. This data can be obtained free of charge via http://www.ccdc.cam.ac.uk/conts/ retrieving.html, or from the Cambridge Crystallographic Data Centre, 12 Union Road, Cambridge CB2 1EZ, UK; fax: (+44) 1223-336-033; or e-mail: deposit@ccdc.cam.ac.uk.

References

[1] A.A.Khandar, V.T.Yilmaz, F.Costantino, S.Gumus, S.A.Hosseini-Yazdi, G. Mahmoudi, Inorganica Chimica Acta 394 (2013) 36–44.

[2] S.J.Sabounchei, H.Nemattalab, S.Salehzadeh, M.Bayat, H.R.Khavasi, H.Adams, Journal of Organometallic Chemistry 693 (2008) 1975–1985.

[3] F.Mendizabal, D.Burgos, C.Olea-Azar, Chemical Physics Letters 463 (2008) 272–277.

[4] B.Moulton, M.J.Zaworotko, Chem. Rev. 101 (2001) 1629-1658.

[5] L.Carlucci, G.Ciani, D.M.Proserpio, Coord.Chem. Rev. 246 (2003) 247-289.

[6] D.Braga, L.Brammer, N.R.Champness, Cryst.Eng.Comm. 7 (2005) 1-19.

[7] S.Kitagawa, R.Matsuda, Coord.Chem. Rev. 251 (2007) 2490-2509.

[8] C.Hu, I.Kalf, U.Englert, Cryst.Eng.Comm. 9 (2007) 603-610.

[9] R.J.Crutchley, Coordination Chemistry Reviews 219–221 (2001) 125–155

[10] E.W.Ainscough, A.M.Brodie, R.J.Cresswell, J.C.Turnbull, J.M.Waters Croatica Chemica Acta 72 (1999) 377-394.

[11] H.Brand, P.Mayer, A.Schulz, T.Soller, A.Villinger, Chem. Asian. J. 3(2008)1050 – 1058.

[12] R.J.Letcher, W.Zhang, C.Bensimon, R.J.Crutchley, Inorg.chimica. Acta 20(1993)183-191.

[13] A.M.Florea, D.Busselberg, BioMetals. 19 (2006) 419-427.

[14] Stoe & Cie, X-AREA, version 1.30: Program for the Acquisition and Analysis of Data, Stoe & Cie GmbH, Darmatadt, Germany, 2005.

[15] Stoe & Cie, X-RED, version 1.28b: Program for Data Reduction and Absorption Correction, Stoe & Cie GmbH, Darmatadt, Germany, 2005.

[16] G.M.Sheldrik, SHELX97. Program for Crystal Structure Solution and Refinement, University of Gottingen, Germany, 1997.

[17] Stoe & Cie, X-SHAP, version 2.05: Program for Crystal Optimization for Numerical Absorption Correction, Stoe & Cie GmbH, Darmatadt, Germany, 2004.

[18] Gaussian 09, Revision A.1, M. J. Frisch, et al. Gaussian, Inc., Wallingford CT, 2009.

[19] E.D.Glendening, A.E. Reed, E.J.Carpenter, F.Weinhold, NBO Version 3.1, 2005.

[20] S.Mietrus, E.Scrocco, J. Chem. Phys. 55 (1981) 117-122.

[21] KF.Barker, J. Clin. Pharmacol. 48(1999)109–124.

[22] Y.Li,P. Leung, L.Yao,Q.W.Song, E. Newton, J. Hosp. Infect. 62(2006)58–63.

[23] Q.L.Feng, J.Wu, G.Q.Chen, F.Z.Cui, T.N.Kim, J.O.Kim, J. Biomed. Mater. Res. 52(2000)662-668.

[24] M. Silverstein, F.X. Webster, Spectrometric Identification of Organic Compounds, sixth ed., John Wiley, Asia, 2003.

[25] J.Vicente, A.Arcas, J.M.Fernandez-Hernandez, D.Bautista, Organometallics, 27(2008) 3978–3985.

[26] K. Nakamoto, Infrared and Raman Spectra of Inorganic and Coordination Compounds, Wiley, New York, 1978.

[27] J.B.King, M.R.Haneline, M.Tsunoda, F.P.Gabbai, J. AM. CHEM. SOC., 124 (2002) 9350-9351.

[28] A.B.P.Lever, Inorganic Electronic Spectroscopy, Elsevier publishing Co., Amsterdam (1984).

[29] H. Hadadzadeh, A.R.Rezvani, F.Belanger-Gariepy, Journal of Molecular Structure 740 (2005) 165–168

[30] F.H.Allen, O.Kennard, D.G.Watson, L.Brammer, A.G.Orpen, J.Chem. Soc. Perkin Trans. II (1987) S1-S19.

[31] E.López-Torres, M.A.Mendiola, J.Organomet.Chem. 725 (2013) 28-33

[32] G.B.Deacon, P.W.Felder, P.C.Junk, K. Müller-Buschbaum, T.J.Ness, C.C.Quitmann, Inorg.chimica. Acta 358(2005) 4389-4393

[33] P.Pyykko,M.Straka, Phys. Chem. Chem. Phys. 2(2000) 2489-2493.

[34] S.C.Nyburg, C.H.Faerman, Acta Crystallogr., Sect. B 41(1985) 274-279.

[35] I.Fleming, Frontier Orbitals and Organic Chemical Reactions, Wiley, London,1978.

[36] M.M.El-Nahass, M.A.Kamel, A.F.El-Deeb, A.A.Atta, S.Y.Huthaily, Spectrochim. Acta A 79 (2011) 1499–1504.

[37] K.Dedachi, T.Hirakawa, S.Fujita, M.T.H.Khan, I.Sylte, N.Kurita, J.Comput. Chem. 32 (2011) 3047–3057.

[38] N.S.Gwaram, H.M.Ali, H.Khaledi, M.A.Abdulla, A.H.A.Hadi, T.K.Lin, C.L.Ching, C.L.Ooi, Molecules 17(2012) 5952-5971.

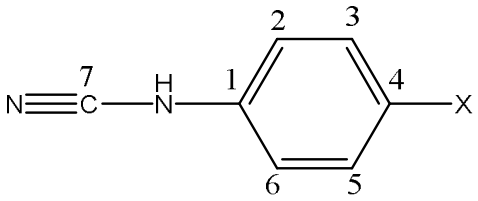

Scheme1. X= -NO_2, -Cl, -Br

Table1. Crystallographic data for **1**.

	1
Empirical Formula	$C_{10}H_9HgN_3O_3$
Formula weight	419.79
T/K	298 (2) K
Crystal system	Monoclinic
Space group	$P2_1$
a/Å	13.1294 (8)
b/Å	9.0851 (5)
c/Å	10.8288 (7)
α/°	90.00
β/°	94.01
γ/°	90.00
V/Å^3	593.5 (2)
Z	2
μ (mm^{-1})	12.97
D_{cal}/Mg m^{-3}	2.349
F(000)	388
*Θ*Range/°	2.5–29.2
Independent reflections	3183
Data/restraints/parameters	3183/0/156
Goodness-of-fit on F^2	1.13
Final *R* indices	$R_1 = 0.0743$, $wR_2 = 0.1925$
R indices (all data)	$R_1 = 0.0840$, $wR_2 = 0.2059$
Largest difference peak and hole (e Å^{-3})	5.08 ,-7.16

Table2. Infrared spectra of the anion of ligands and the complexes of **1** – **3** (cm^{-1}).

4-NO_2pcyd$^-$	**1**	4-Clpcyd$^-$	**2**	4-Brpcyd$^-$	**3**	Assigments
1150,1295	1125	1185,1245	1165	1260,1100	1070	ν(C–N)
2145	2140	2194	2190	2186	2183	ν(C≡N)
1597.7 1337.4	1590.0 1310.4					ν(NO_2)
	1726.3		1728.2		1725.4	ν(CO)

Table3. ^{1}H-NMR of ligands and the complexes of **1**-**3** (ppm).

Observed protons	4-NO_2pcyd	**1**	4-Clpcyd	**2**	4-Brpcyd	**3**
Phenyl	7.06(d) 7.92(d)	6.82(d) 7.62(d)	6.91(d) 7.28(d)	6.65(d) 6.98(d)	6.91(d) 7.28(d)	6.68(d) 7.14(d)
-CH_3		1.18(s)		1.15(s)		1.16(s)
-CH_2		2.61(d) 2.14(d)		2.49(d) 2.12(d)		2.57(d) 2.10(d)

d (doublet), s (singlet)

Table4. ^{13}C-NMR of ligands and the complexes of **1**-**3** (ppm).

Observed carbons	4-NO_2pcyd	**1**	4-Clpcyd	**2**	4-Brpcyd	**3**
C(H_3)		30.2		30.2		30.2
C(H_2)		56.4		56.4		56.3
C_7	112.5	120.1	111.7	119.0	100.7	107.6
$C_{2,6}$	120.0	124.1	116.9	120.1	115.5	121.0
C_4	129.0	126.7	128.9	126.6	128.6	126.4
$C_{3,5}$	132.5	131.9	129.9	128.7	132.1	131.6
C_1	136.6	153.0	136.2	152.7	135.5	151.9
C(=O)		216.9		216.6		216.1

Table5. Electronic absorption data for $[Hg(CH_2COCH_3)L]_n$ complexes.

L	Experimental	Calculated	Assignment
	λ_{max}(log ε)[a]	λ_{max}(*f*)[b]	
4-NO_2pcyd	451(3.85)	446(0.0195)	π→π*
	267(3.18)	274(0.024)	π→π*
4-Clpcyd	418(3.98)	–	π→π*
	267(3.58)	–	π→π*
4-Brpcyd	404(4.17)	–	π→π*
	266(3.97)	–	π→π*

[a] λ in nm (log ε), in DMF solution.

[b] the oscillator strength (*f*)

Table6. Selected bond lengths (Å) and bond angles (˚) for the compound **1**.

Bond lengths	
N(1)-C(1)	1.17(2)
N(2)-C(1)	1.29(2)
N(2)-C(2)	1.37(2)
N(3)-C(5)	1.39(3)
Hg(1)-N(2)	2.120(17)
Hg(1)-C(8)	2.097(19)
Hg(1)-O(3)	2.820 (17)
Bond angles	
C(8)-Hg(1)-N(2)	175.6(7)
C(1)-N(2)-C(2)	118.8(17)
C(1)-N(2)-Hg(1)	116.2(13)
C(2)-N(2)-Hg(1)	124.2(13)
N(1)-C(1)-N(2)	174(2)
H(8A)-C(8)-H(8B)	108.2
C(9)-C(8)-H(8A)	109.7
C(9)-C(8)-H(8B)	109.7
Hg(1)-C(8)-H(8B)	109.7
Hg(1)-C(8)-H(8A)	109.7
C(9)-C(8)-Hg(1)	110.0(13)

Table7. A comparison between the selected calculated bond lengths (Å) and bond angles (˚) and corresponding experimental values for **1**.

	b1	b2	X-ray
Bond lengths (Å)			
N(1)-C(1)	1.161	1.193	1.17(2)
C(1)-N(2)	1.381	1.269	1.29(2)
N(2)-C(2)	1.436	1.420	1.37(2)
N-Hg	2.076	2.013	2.120(17)
Bond angles (˚)			
N(1)-C(1)-N(2)	178.3	171.1	174(2)
C(1)-N(2)-C(2)	116.0	120.8	118.8(17)
Hg-N-C(2)	116.3	176.6	124.2(13)
C(1)-N(2)-C(2)-C(3)	0.0	0.0	---

Table8. Calculated NBO charges on selected atoms of ligand (4-NO_2pcyd) and isomers of complex **1**.

	a	b1	b2
N1	-0.337	-0.198	-0.317
C1	0.089	0.126	0.252
N2	-0.362	-0.314	-0.271
C2	0.114	0.137	0.12
Hg	------	0.234	0.197

Table9. Most important occupancies of NBOs in atomic units (LP: lone pair)

b1			b2		
donor	acceptor	energy	donor	acceptor	energy
N2(LP)	Hg	105.88	N1(LP)	Hg	90.73
N2(LP)	σ*(Hg-C)	46.21	N1(LP)	σ*(Hg-C)	16.48

Table10. Inhibition zone values from disk diffusion tests for free ligand of 4-NO_2pcyd and the complex **1**.

Inhibition zone diameter (mm)		Compound
Salmonella	*Ecoli*	
> 30 mm	> 30 mm	4-NO_2pcyd
> 30 mm	> 30 mm	**1**

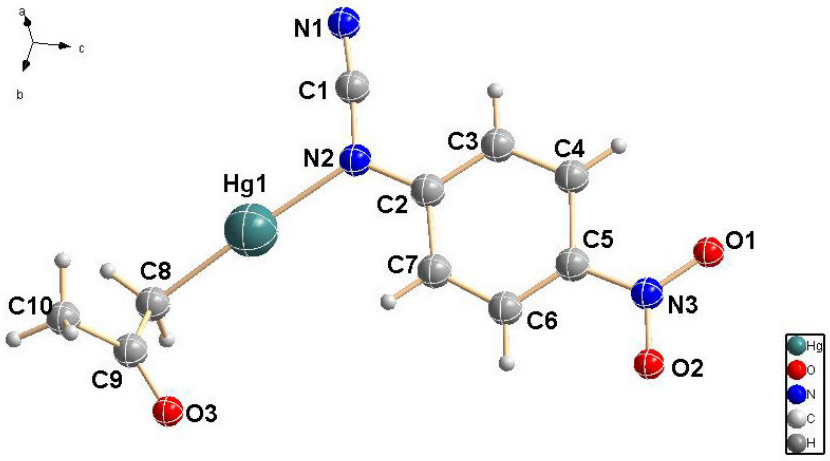

Fig.1. ORTEP structure of the $[Hg(CH_2COCH_3)(4\text{-}NO_2pcyd)]_n$ complex.

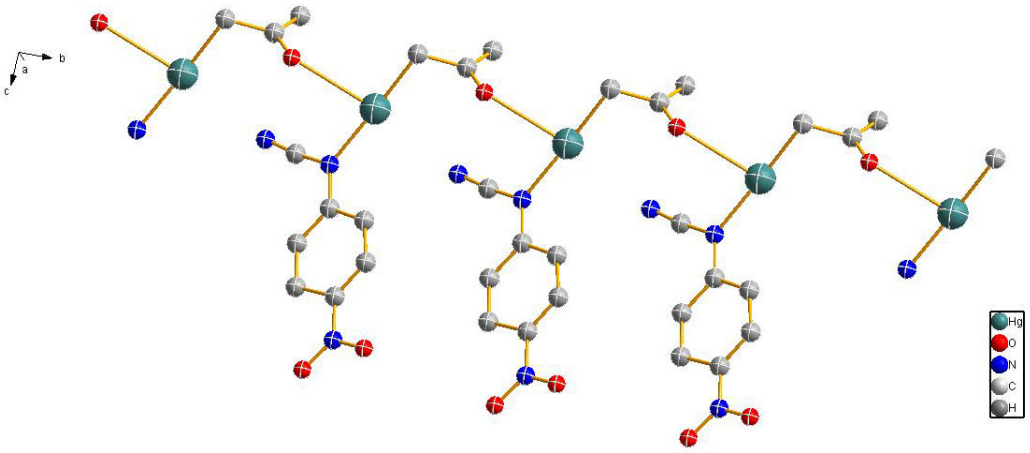

Fig.2. Projection of the crystal packing down the b-axis

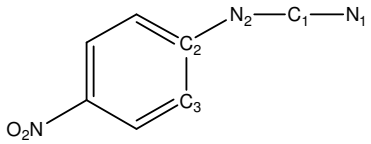

Numbering scheme

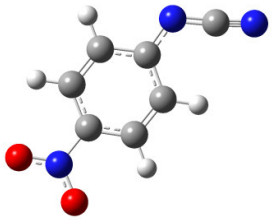

a

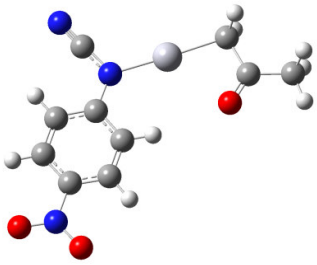

b1

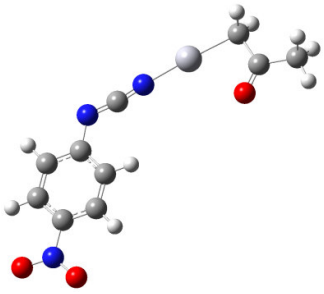

b2

Fig.3. Numbering scheme and optimized structures of ligand (4-NO_2pcyd) (a) and both isomers of complex **1** (b1, b2).

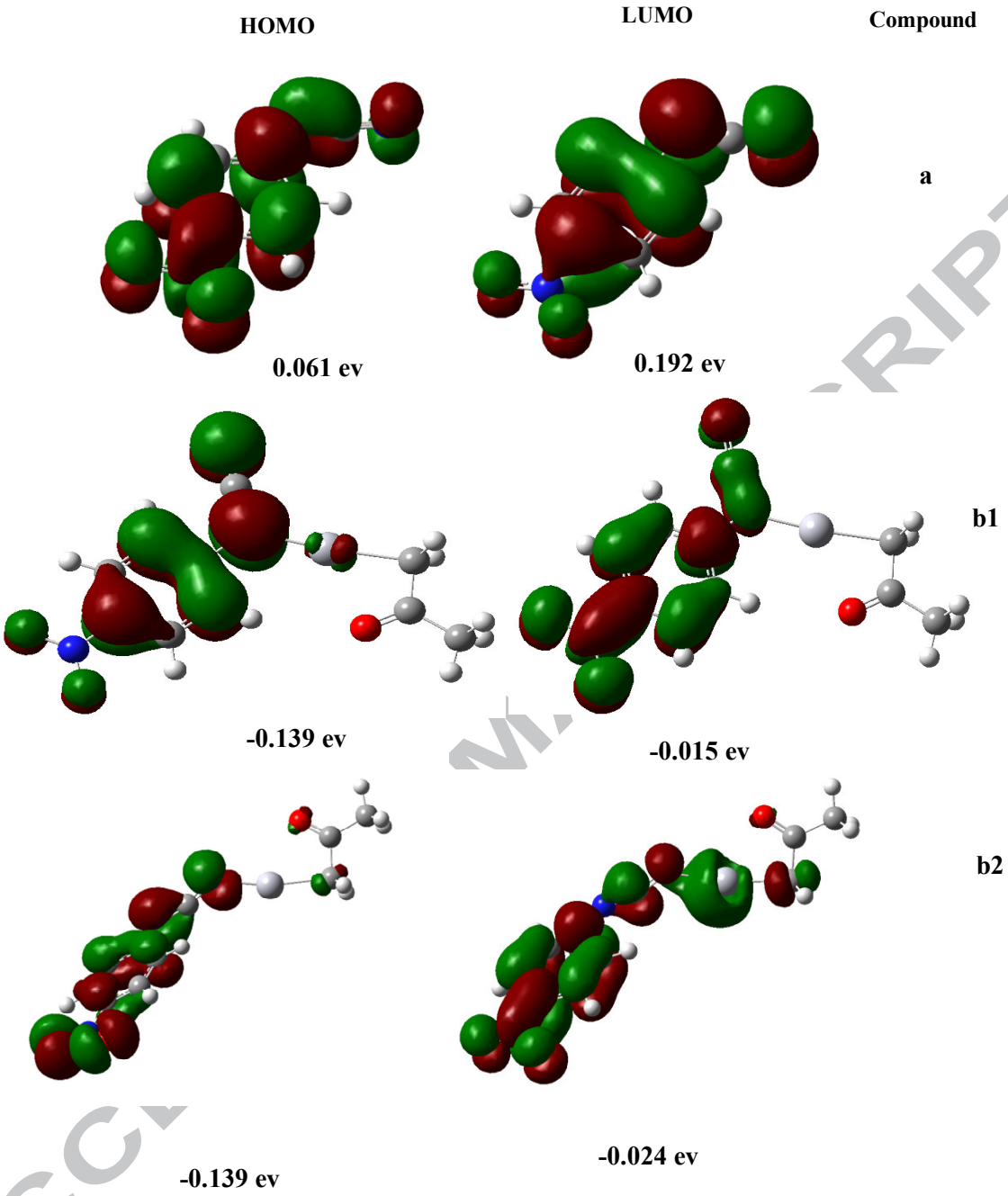

Fig.4. Graphical presentation of calculated frontier orbitals of ligand (4-NO_2pcyd) before (a) and after binding to Hg (II) as two isomers (b1 and b2) of complex **1** and their energies.

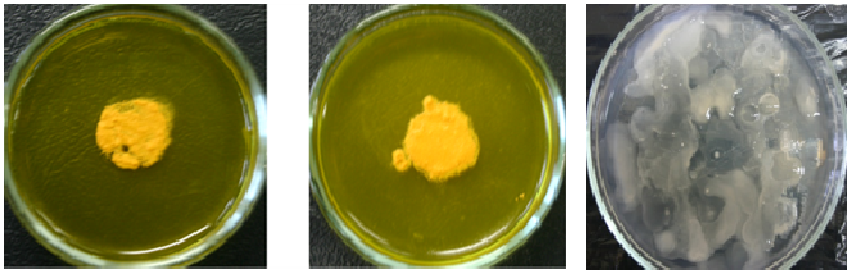

Fig.5. The disc diffusion test showing completely inhibition of Ecoli (left) and Salmonella (middle) by the complex**1** in Petri plates (d>30 mm) compared to negative control (right) showing a white slimy texture of bacterial growth.

►New mercury (II) polymers with phenylcyanamide ligand were prepared and characterized.
►The single crystal X-ray analysis reveals phenylcyanamide ligand is coordinated to Hg (II) through an amine nitrogen.
►As shown by DFT calculations, the experimentally determined structure is more stable than other bonding modes.
►The compounds show antibacterial activities against Gram-negative and -positive bacteria.

Syntheses, studies and crystal structure of new coordination polymers of mercury (II) with phenylcyanamide derivative ligands

Hossein Chiniforoshan[*a], Nasimeh Pourrahim [a], Leila Tabrizi [a], Hossein Tavakol [a], Mohammad R. Sabzalian [b].

[a]*Department of Chemistry, Isfahan University of Technology, Isfahan 84156-83111, Iran*
[b]*Department of Agronomy and Plant Breeding, College of Agriculture, Isfahan University of Technolog*

We report syntheses and study a series of mercury (II) compounds with phenylcyanamide derivative ligands which coordinated to Hg (II) through amine nitrogen alone for the first time. Also, theoretical methods and antibacterial activities have been studied.

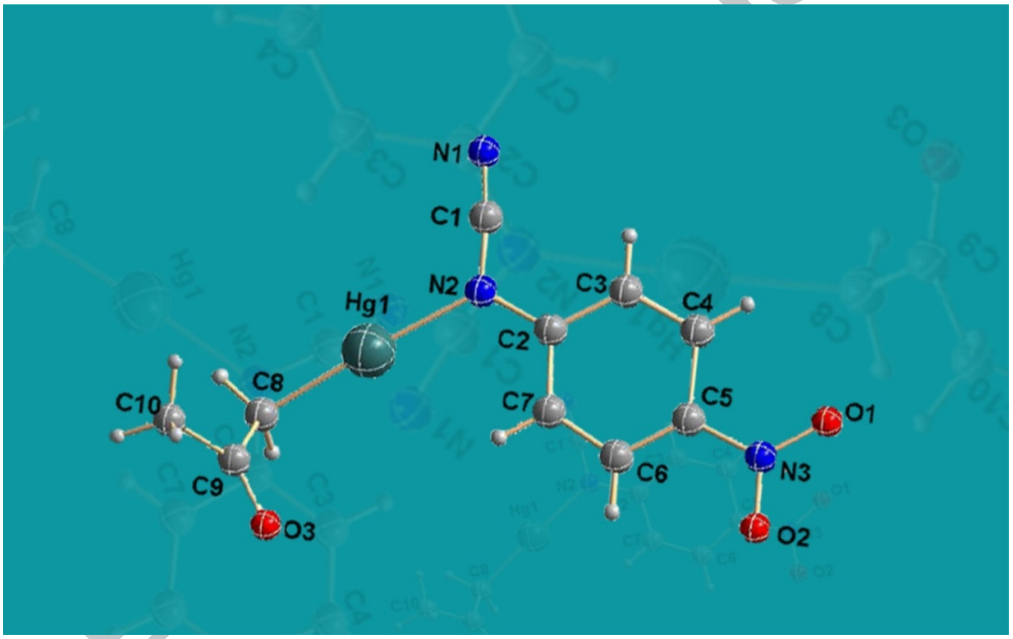

*Corresponding author: H. Chiniforoshan; Email: Chinif@cc.iut.ac.ir
Tel: +983113913261; fax: +983113912350